Master of Science Thesis in Electrical Engineering
Department of Electrical Engineering, Linköping University, 2020

Efficient Route Optimization for UAVs in Maritime Search and Rescue

Tobias Fridén

LINKÖPING
UNIVERSITY

Master of Science Thesis in Electrical Engineering

Efficient Route Optimization for UAVs in Maritime Search and Rescue:

Tobias Fridén

LiTH-ISY-EX--YY/NNNN--SE

Supervisor: **Jonatan Olofsson**
ISY, Linköpings universitet
Fredrik Falkman
Airpelago

Examiner: **Daniel Axehill**
ISY, Linköpings universitet

Division of Automatic Control
Department of Electrical Engineering
Linköping University
SE-581 83 Linköping, Sweden

Sammanfattning

Det här som vi har hållit på med är jätteviktigt faktiskt och det vi gjort blev bara såååå bra. Kanske inte helt otippat, men det glass är såååå gott!

Förresten har vi blivit bäst på att skriva rapporter, så nu ska ska vi inte gå in närmare på några detaljer såhär i sammanfattningen.

Abstract

If your thesis is written in English, the primary abstract would go here while the Swedish abstract would be optional.

Contents

Notation

Några mängder

Notation	Betydelse
$\mathbb{N}$	Mängden av naturliga tal
$\mathbb{R}$	Mängden av reella tal
$\mathbb{C}$	Mängden av komplexa tal

Förkortningar

Förkortning	Betydelse
ARMA	Auto-regressive moving average
PID	Proportional, integral, differential (regulator)

1
Theory

In the following chapter, the necessary theory will be presented.

1.1 Wind

Wind can have large effects on mission execution duration and energy consumption, and as such a reliable wind model is necessary to calculate an efficient route.

Many authors have studied wind modeling in UAV as well as general airspace applications. A method for online wind field features such as shear and gust is presented in [6]. Uncertainty in wind can be handled by choosing the worst case scenario for energy consumption, creating a robust model [9]. Meteorological forecast data can be represented by a continuous function by creating regression models for the north-south and east-west components. This approach is used in route optimization for commercial aircraft [8].

Since the route optimization is performed offline in this thesis, the focus is on methods to predict the wind field using the current meteorological forecast and data collected from previous flights in the same geographical area.

1.1.1 Spatial interpolation

Spatially distributed phenomena sampled on a grid can be interpolated using *spatial interpolation* methods [3].

Definition 1.1 (Spatial interpolation). Given N values of a studied phenomenon $z_1, \ldots, z_N$ measured at discrete points $\boldsymbol{r}_j = (x_{1,j}, \ldots, x_{d,j}$, $j = 1, \ldots, N$ on a d-dimensional grid, the spatial interpolation $F(\boldsymbol{r})$ fulfills

$$F(\boldsymbol{r}_j) = z_j, \quad j = 1, \ldots, N \tag{1.1}$$

This approach can further be divided into three categories, *local neighbourhood*, *geostatistical* and *variational* methods.

Local neighbourhood methods interpolate the value in a given point by calculating a weighted average of all or a fixed subset of the sample points. One commonly used such method is *Inverse Distance Weighted Interpolation* (IDW). Such methods are easily implemented but has some well known shortcomings.

Geostatistical methods represent the sampled values as one realisation of a random function with a certain spatial covariance. One commonly used method is *Kriging*. This approach is often successful when the statistical properties of the observed phenomenon is of important value. It has shown to be less efficient when local geometry and smoothness are important.

Variational methods aim to find a function which passes through or close to the points z_i while being as smooth as possible. The resulting function can be represented as

$$F(\boldsymbol{r}) = T(\boldsymbol{r}) + \sum_{j=1}^{N} \lambda_j R(\boldsymbol{r}, \boldsymbol{r}_j) \tag{1.2}$$

where $T(\boldsymbol{r})$ is a linear trend function and $R(\boldsymbol{r}, \boldsymbol{r}_j)$ is a radial function depending on the choice of smoothness norm. As long as the radial function is smooth, $F(\boldsymbol{r})$ is also smooth which is often a requirement for usage in optimization problems.

1.1.2 Thin Plate Splines

TPS is a commonly used method for variational spatial interpolation. In two dimensions, this method has the physical interpretation of fitting a thin metal sheet at all data points while minimizing the bending energy. A thorough presentation of TPS and the underlying theory is given in [2]. The necessary results for the application in this thesis are presented below.

The 3-dimensional TPS interpolator minimizes

$$\frac{1}{N}\sum_{j=1}^{N}(z_i - f(\boldsymbol{r}_i))^2 + \lambda J(f) \tag{1.3}$$

where λ is a smoothing parameter and

$$J(f) = \int_{-\infty}^{\infty}\int_{-\infty}^{\infty}\int_{-\infty}^{\infty}(f_{x_1x_1}^2 + f_{x_2x_2}^2 + f_{x_3x_3}^2 + 2[f_{x_1x_2}^2 + f_{x_2x_3}^2 + f_{x_1x_3}^2])dx_1dx_2dx_3 \tag{1.4}$$

is the TPS smoothness penalty functional.

The solution that minimizes (1.3) is given by the system of equations

$$z_j = f(\boldsymbol{r}_j) = \left(b_0 + \sum_{k=1}^{3} b_k x_{k,j}\right) + \sum_{i=1}^{N} w_i G(\boldsymbol{r}_i, \boldsymbol{r}_j) + \lambda w_j, \quad j = 1, \ldots, N \tag{1.5}$$

where $G(\boldsymbol{r}_i, \boldsymbol{r}_j)$ is a Green's function depending on the data dimension. In the 3-dimensional case, it is given by

$$G(\boldsymbol{r}_i, \boldsymbol{r}_j) = -\frac{1}{8\pi}|\boldsymbol{r}_i - \boldsymbol{r}_j| \tag{1.6}$$

Define $\boldsymbol{z} = (z_1, \ldots, z_N)^T$, $\boldsymbol{b} = (b_0 \ldots b_d)^T$, $\boldsymbol{w} = (w_1 \ldots w_N)^T$ and the matrices K and L where $K_{i,j} = G(\boldsymbol{r}_i, \boldsymbol{r}_j)$ and the i-th row of $L = (1 \quad \boldsymbol{r}_i^T)$. The linear term in (1.5) lies in the null space of $J(f)$ so

$$L^T \boldsymbol{w} = 0 \tag{1.7}$$

Equations (1.5) and (1.7) can be written on matrix form as

$$\begin{pmatrix} K + \lambda I & L \\ L^T & 0 \end{pmatrix}\begin{pmatrix} \boldsymbol{w} \\ \boldsymbol{b} \end{pmatrix} = \begin{pmatrix} \boldsymbol{z} \\ 0 \end{pmatrix} \tag{1.8}$$

which has a closed form solution if L is of full rank.

1.1.3 Wind Modeling using TPS

The Swedish Meteorology and Hydrology Institute (SMHI) use Numerical Weather Prediction (NWP) to forecast weather conditions four times a day on a 2.5×2.5

km grid with 65 altitude levels. However, this model does not capture wind variations on a scale smaller than 2.5 km which might be relevant for UAV route optimization.

The actual wind vector in an arbitrary coordinate (λ, ϕ) and altitude h is decomposed as

$$\boldsymbol{w}(\lambda, \phi, h) = \boldsymbol{w}_F + \boldsymbol{w}_B \tag{1.9}$$

where $\boldsymbol{w}_F$ is the forecasted wind vector for this grid cell and $\boldsymbol{w}_B$ is the wind bias in the given coordinate.

To derive the wind model, the following assumptions are made.

Assumption 1.2. The UAV altitude is constant during the entire route, which implies that wind variations depending on altitude can be excluded from the wind model.

Assumption 1.3. The wind magnitude $W = |\boldsymbol{w}|$ and direction $\theta_w = \operatorname{Arg} \boldsymbol{w}$ are uncorrelated.

Assumption 1.4. The wind bias vector is dependent on the coordinate (λ, ϕ) and wind forecast $\boldsymbol{w}_F$, i.e.

$$\boldsymbol{w}_B = f(\lambda, \phi, \boldsymbol{w}_F) \tag{1.10}$$

Given these assumptions, the wind model can be defined.

Definition 1.5 (Wind model). The wind vector $\boldsymbol{w}(\lambda, \phi)$ is modelled as

$$\boldsymbol{w} = W(\cos\theta_w, \sin\theta_w) \tag{1.11}$$

where

$$\begin{cases} W = |\boldsymbol{w}_F| + f_W(\lambda, \phi, |\boldsymbol{w}_F|) \\ \theta_w = \operatorname{Arg} \boldsymbol{w}_F + f_\theta(\lambda, \phi, \operatorname{Arg} \boldsymbol{w}_F) \end{cases} \tag{1.12}$$

in which f_W and f_θ are TPS interpolators for the bias in wind magnitude and direction.

1.1.4 Data collection and model evaluation

To create and evaluate the wind model, real flight data has to be collected. By equipping the UAV with a *pitot probe*, the actual wind can be measured as

$$\boldsymbol{w} = \boldsymbol{v} + \boldsymbol{v}_a \tag{1.13}$$

where $\boldsymbol{v}$ is the ground speed measured by GPS and $\boldsymbol{v}_a$ is the airspeed [7]. The current wind forecast $\boldsymbol{v}_F$ is obtained from SMHI [1]. By collecting N measurements from different coordinates and wind conditions, the interpolation points are

$$\begin{cases} z_j = |\boldsymbol{w}_j| - |\boldsymbol{w}_F| \\ \boldsymbol{r}_j = (\lambda_j, \phi_j, |\boldsymbol{w}_F|) \end{cases} \quad j = 1, \dots, N \tag{1.14}$$

for the magnitude bias and

$$\begin{cases} z_j = \operatorname{Arg} \boldsymbol{w}_j - \operatorname{Arg} \boldsymbol{w}_F \\ \boldsymbol{r}_j = (\lambda_j, \phi_j, \operatorname{Arg} \boldsymbol{w}_F) \end{cases} \qquad j = 1, \ldots, N \tag{1.15}$$

for the direction bias. Using these data points, f_W and f_θ can be calculated as defined in (1.8).

1.2 UAV dynamics

A suitable model of the UAV dynamics has to be derived in order to calculate an efficient route. The UAV uses the L_1 control law presented in [5]. This control law navigates from the origin to a goal coordinate by steering towards a reference point P along the line from the origin to the goal which is at distance L_1 from the UAV in each time step. Based on this control law, some initial assumptions are made and the UAV state and control vectors are defined.

Assumption 1.6. The UAV will always hold a constant altitude, which means that the route optimization can be performed in two dimensions without taking altitude into account.

Assumption 1.7. The UAV is able to hold a constant velocity V relative to the surrounding air. Any internal dynamics related to velocity are neglected.

Definition 1.8 (UAV state). The UAV state vector is defined as

$$\boldsymbol{x} = (\lambda, \phi, \theta) \tag{1.16}$$

where (λ, ϕ) is the latitude and longitude coordinate and θ is the current heading, defined to be zero in the north direction.

Definition 1.9 (UAV control). The UAV control vector is defined as

$$\boldsymbol{u} = (\lambda_g, \phi_g, V) \tag{1.17}$$

where (λ_g, ϕ_g) is the latitude and longitude of the desired goal position and V is the desired velocity.

To derive the state-space model, the following variables are defined:

$$\begin{cases} \boldsymbol{v} = V(\sin\theta, \cos\theta) \\ \boldsymbol{r} = (\lambda, \phi) \\ \boldsymbol{g} = (\lambda_g, \phi_g) \\ \theta_g = \mathrm{atan2}(\lambda_g, \phi_g) \\ d = (\boldsymbol{r} \times \boldsymbol{g}/|\boldsymbol{g}|) \cdot \hat{\boldsymbol{z}} = -\lambda \sin\theta_g + \phi\cos\theta_g \end{cases} \tag{1.18}$$

where $\boldsymbol{v}$ is the UAV velocity vector, $\boldsymbol{r}$ is the UAV position, $\boldsymbol{g}$ is the goal position, θ_g is the goal heading and d is the cross track error. All the defined variables are shown in Figure 1.1.

In the ArduPilot implementation, the distance L_1 is calculated as

$$L_1 = \begin{cases} \frac{1}{\pi}\zeta\Delta T V & \text{if} \quad |\frac{1}{\pi}\zeta\Delta T V| > |\boldsymbol{r} - \boldsymbol{g}| \\ |\boldsymbol{r} - \boldsymbol{g}| & \text{otherwise} \end{cases} \tag{1.19}$$

where ζ is the damping factor and ΔT is the update period of the controller [4].

In each time step, the control law corresponds to following a circular segment with radius

$$R = \frac{L_1}{2\sin\eta} \tag{1.20}$$

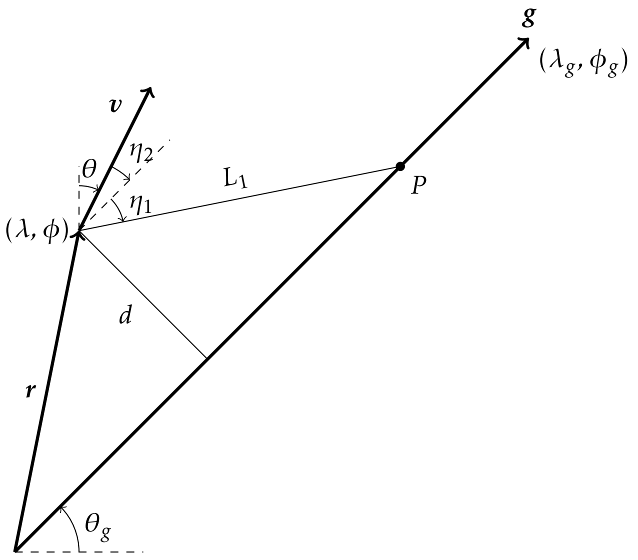

Figure 1.1: *Definition of UAV State Space variables*

which is tangent to $\boldsymbol{v}$ in (λ, ϕ). η is defined as the angle between the UAV velocity vector $\boldsymbol{v}$ and the line from the UAV to P. The centripetal acceleration is then

$$a_s = 2\frac{V^2}{L_1}\sin\eta \tag{1.21}$$

By introducing a line dividing η which is parallel to $\boldsymbol{g}$ it can be written as $\eta = \eta_1 + \eta_2$ where η_1 is the angle between this line and the line between the UAV and P, and η_2 is the angle between $\boldsymbol{v}$ and this line. If the magnitude of η is small

$$\sin\eta \approx \eta = \eta_1 + \eta_2 \tag{1.22}$$

where

$$\eta_1 \approx \frac{d}{L_1} \tag{1.23}$$

and

$$\eta_2 \approx \frac{\dot{d}}{V} \tag{1.24}$$

From the definition of d,

$$\dot{d} = -\dot{\lambda}\sin\theta_g + \dot{\phi}\cos\theta_g = V(-\sin\theta\sin\theta_g + \cos\theta\cos\theta_g) \tag{1.25}$$

By combining equations (1.22)-(1.24), the centripetal acceleration can then be approximated as

$$a_s \approx 2\frac{V}{L_1}\left(\dot{d} + \frac{V}{L_1}d\right) \tag{1.26}$$

From the laws of circular motion the angular velocity is given by

$$\dot{\theta} = \frac{a_s}{V} \tag{1.27}$$

The UAV state-space model can now be defined by combining equations (1.16)-(1.27).

Definition 1.10 (UAV State-Space model). The UAV state-space model is defined as

$$\dot{\boldsymbol{x}} = f(\boldsymbol{x}, \boldsymbol{u}) \tag{1.28}$$

where

$$f(\mathbf{x}, \mathbf{u}) = \begin{bmatrix} V \sin\theta \\ V \cos\theta \\ \frac{2}{L_1}\left(\dot{d} + \frac{V}{L_1} d\right) \end{bmatrix} \tag{1.29}$$

with d and θ_g as defined in (1.18), $\dot{d}$ as defined in (1.25) and L_1 as defined in (1.19).

Bibliography

[1] Smhi open data api, 2019. URL `https://opendata.smhi.se/`.

[2] Technisch-Naturwissenschaftliche Fakultät. Efficient thin plate spline interpolation and its application to adaptive optics. 2010.

[3] L Mitas and H Mitasova. Spatial Interpolation. 2005.

[4] Ardupilot: The open source autopilot. Arduplane: Navigation tuning, 2019. URL `http://ardupilot.org/plane/docs/navigation-tuning.html#tuning-waypoint-transition-behaviour`.

[5] Sanghyuk Park, John Deyst, and Jonathan How. *A New Nonlinear Guidance Logic for Trajectory Tracking*. doi: 10.2514/6.2004-4900. URL `https://arc.aiaa.org/doi/abs/10.2514/6.2004-4900`.

[6] L. Rodriguez, J. A. Cobano, and A. Ollero. Wind field estimation and identification having shear wind and discrete gusts features with a small uas. In *2016 IEEE/RSJ International Conference on Intelligent Robots and Systems (IROS)*, pages 5638–5644, Oct 2016. doi: 10.1109/IROS.2016.7759829.

[7] L. Rodríguez, F. Balampanis, J. A. Cobano, I. Maza, and A. Ollero. Energy-efficient trajectory generation with spline curves considering environmental and dynamic constraints for small uas. In *2017 IEEE/RSJ International Conference on Intelligent Robots and Systems (IROS)*, pages 1739–1745, Sep. 2017. doi: 10.1109/IROS.2017.8205987.

[8] Manuel Soler. *Comercial aircraft trajectory planning based on multiphase mixed-integer optimal control*. Omm Editorial, 2013.

[9] Chien-Ming Tseng, Chi-Kin Chau, Khaled Elbassioni, and Majid Khonji. Autonomous Recharging and Flight Mission Planning for Battery-operated Autonomous Drones. *arXiv e-prints*, art. arXiv:1703.10049, Mar 2017.

Index